Vehicle crashworthiness performance in frontal impact: Mathematical model using elastic pendulum

Gulshan Noorsumar *, Svitlana Rogovchenko, Kjell G. Robbersmyr, Dmitry Vysochinskiy

Faculty of Engineering and Science, University of Agder, Jon Lilletuns vei 9, Grimstad, 4876, Norway

ARTICLE INFO

ABSTRACT

Vehicle occupant injuries due to collisions cause many fatalities every year. Safe vehicle design plays a critical role in averting serious injuries to occupants and vulnerable road users in the event of a crash. In this paper we study a full frontal vehicle crash against a rigid barrier introducing a Lumped Parameter Model (LPM) inspired by the elastic pendulum motion. The model uses polar coordinates to simplify the problem and the governing equations have been defined using Lagrangian formulation. The Simulink model has been validated against Finite Element (FE) data demonstrating good correlation with pitching angle and maximum crush of the vehicle. These parameters are crucial for designing vehicles which efficiently protect occupants.

1. Introduction

Vehicle collisions are the one of the major causes of occupant injuries in a vehicle crash event. The 2015 European Commission report identifies a frontal impact as the most common crash scenario leading to serious injuries, followed by a side impact. These injuries are caused by different forces acting on the cage protecting the occupants in a collision in various impact scenarios [1,2]. The report also suggests further studies of mechanisms and measures aimed at reducing injury severity in a crash. Factors leading to occupant head and neck injuries are the vehicle pitch and drop in case of a full frontal impact [3]. Occupant interaction with vehicle cage leads to severe injuries in a crash, especially in case of unbelted occupants. In order to prevent head to roof/header contacts it is imperative to include vehicle pitch and drop in design considerations for full frontal impact injury mitigation [3].

The geometry and deformation of the front end members are important for predicting the forward pitching of a vehicle. In fact, downward bending of the rails generated by the imbalance of forces acting on the part in the vertical direction is a key reason for pitching in full frontal impacts [4,5]. The rotation of the vehicle that leads to yawing and rolling is not included in most simulation models predicting the injury response because they are negligible in case of a full frontal impact. Designing an ideal straight frame vehicle safety engineers face challenges due to package constraints (engine compartment); this leads to vertical downward bending of frame rail structures in body-on-frame vehicles during deformation. Such out of plane bending not only causes less efficient energy absorption but also adds a downward moment causing an imbalance of forces acting on the vehicle. The vehicle pitch

was simulated using CAE modeling by Chang et al. who concluded that the modeling and design of vehicle rails play a crucial role in vehicle pitch and drop [6,7]. Vehicle rotations were also predicted by Lumped Parameter Models (LPM) in [4,8] using a 6 DOF (Degrees of Freedom) vehicle model with an active vehicle dynamics control system.

Mathematical modeling is used in vehicle development process to respond to changing safety norms and to ensure that new vehicles are designed to protect pedestrians and occupants in a crash. Mathematical models replace physical testing to predict the injury values in a collision scenario; Finite Element (FE) models have good accuracy in correlating the kinematics of an impact and have been used in several applications in the automotive industry [9,10]. LPMs are usually designed as simplified spring-damper systems representing a deformable part and a rigid lumped mass component replicating the non-deformable occupant compartment. The study by Kamal was one of the first applications of LPM in automotive crashworthiness modeling [11]. In the last decade several researchers employed parameter estimation techniques to study impact dynamics using LPM models [12,13]. Pavlov [14] represented a vehicle as a pendulum in motion and predicted vehicle pitching using an inverted pendulum. Occupant modeling using inverted spherical pendulum model was conducted by Cyrén and Johansson [15], who derived the equations of motion of the pendulum using Lagrangian formulation. Inverted pendulum has also been used in explaining the dynamics of a two-wheeled vehicle with self-tilt motion by Miao [16].

This paper introduces an elastic pendulum model to explain the impact kinematics for a full frontal impact model (0% offset) of a vehicle which is undergoing impact at 56 kmph against a rigid barrier;
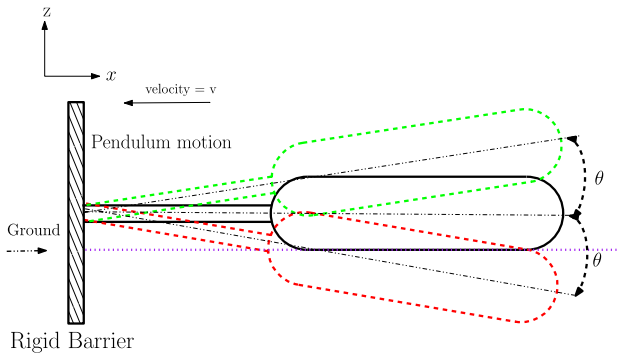
Fig. 1. Vehicle body rotating like a pendulum about the impact point.
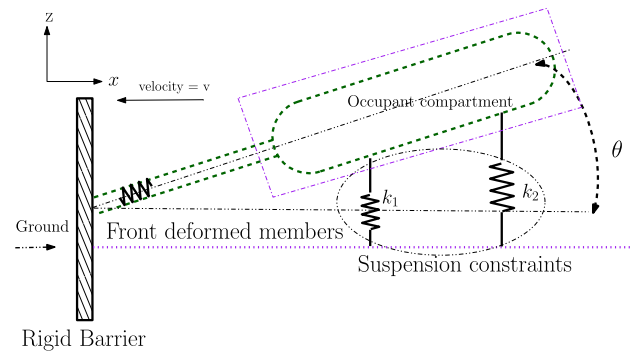

Fig. 2. Elastic pendulum with constraints representing a vehicle under impact.

the vehicle occupant cage is represented by a compound pendulum. The vehicle pitching angles are generally in the range of 5–20 deg making it easier to conduct an energy analysis on the model [17,18]. The equations of motion of the system are derived using the Lagrangian formulation. The model is validated against an FE model simulation, details are explained in the next section.

2. Methodology

Our model represents a non-linear vehicle impact as a pendulum in motion. The vehicle hitting a rigid impactor goes through three stages:

- front end deformation (modeled as in an elastic pendulum),
- rotation about the impact point acting like a pivot in case of a pendulum,
- restoring force due to gravity bringing the vehicle back to the rest position.

Some of the assumptions in the model include [19]:

- Only vehicle rotations about the y-axis (pitching) were considered in the model; rotations in other axes have been neglected.
- Energy losses like friction and heat losses were neglected.
- Although the system behaves non-linearly in a crash, the front-end spring and damper characteristics were assumed to be piece-wise linear with four breakpoints.

The periodic pendulum motion shown in Fig. 1 is adopted for this model; the pendulum is allowed to swing back and forth from its rest position. In the case of the vehicle under impact, the occupant compartment acts like a pendulum bob rotating about the pivot point leading to vehicle pitching. The vehicle is not allowed to swing back and forth due to the ground acting as a constraint. The vehicle suspension system also acts as a constraint to restrict the motion of the pendulum. Fig. 2 shows the model with the constraints, the barrier defined for the LPM is a non deformable 0% offset impactor. The LPM used is a 2 DOF system, similar to the one developed in [5]. The non deformable occupant compartment is represented in the model by the concentrated mass. The deformable front end comprising of vehicle rails, crush cans and the plastic parts is represented by a spring and damper system in Fig. 3.

The vehicle front end undergoes deformation to absorb energy which leads to the deceleration of the vehicle; the time of maximum crush generally coincides with the instant when the vehicle attains zero velocity. The pendulum LPM uses a spring damper system to absorb the impact energy as shown in Fig. 4. In a full frontal impact against a rigid barrier the vehicle starts pitching forward due to the imbalance of forces as explained by Chang et al. [3,6]; this behavior has been replicated in the LPM (Fig. 5) and modeled as an elastic pendulum.
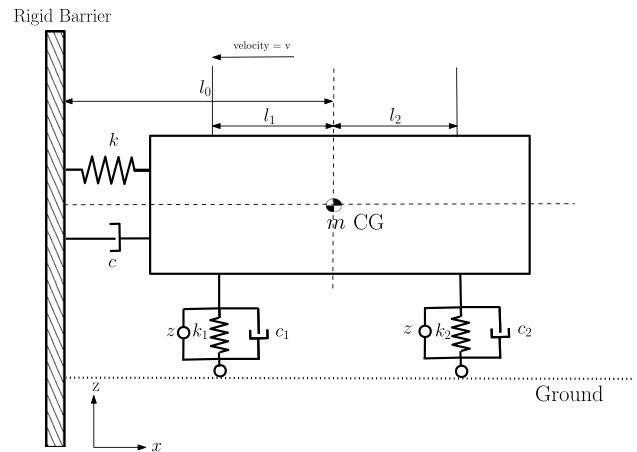

Fig. 3. LPM Model of a vehicle impacting a rigid barrier.

2.1. Finite element (FE) model

The LPM is validated by an FE model similar to that considered in [5]. The FE simulations conducted for a vehicle impact at 56 kmph were used to validate this model. The FE model developed by National Highway Traffic Safety Administration (NHTSA) through the reverse engineering process [20] was used to compare the LPM and FE curves. Parameter identification was conducted to determine the spring and damper characteristics for the non-linear deformation in the vehicle front.

2.2. Parameter identification for front end spring and damper characteristics

The front-end deformation for the vehicle components generally follows non-linear force deformation characteristics. Predicting the behavior of the system has been a challenge for many researchers. This front-end system has been approximated using piece-wise linear spring and damper characteristics. These characteristics for the front-end spring-damper system are derived using the algorithm developed by the authors in [5,21]. The gradient descent optimization algorithm developed in [5] is modified to include deformation and pitching of the vehicle during the entire event of collision. The non-linear force–deformation curve is assumed to be piece-wise linear with six breakpoints in the curve. The stiffness k and spring force F_k are related by Eq. (1). Similarly, the damper coefficient c is related to the damping force F_c by Eq. (2) [17].

$$F_k = k(x) \cdot x, \tag{1}$$

$$F_c = c(\dot{x}) \cdot \dot{x}, \tag{2}$$

where

$$k(x) = \begin{cases} \frac{(k_2-k_1)\cdot|\hat{x}|}{x_1} + k_1, & \text{for } |\hat{x}| \leq x_1, \\[2mm] \frac{(k_3-k_2)\cdot(|\hat{x}|-x_1)}{(x_2-x_1)} + k_2, & \text{for } x_1 \leq |\hat{x}| \leq x_2, \\[2mm] \frac{(k_4-k_3)\cdot(|\hat{x}|-x_2)}{(x_3-x_2)} + k_3, & \text{for } x_2 \leq |\hat{x}| \leq x_3, \\[2mm] \frac{(k_5-k_4)\cdot(|\hat{x}|-x_3)}{(x_4-x_3)} + k_4, & \text{for } x_3 \leq |\hat{x}| \leq x_4, \\[2mm] \frac{(k_6-k_5)\cdot(|\hat{x}|-x_4)}{(x_5-x_4)} + k_5, & \text{for } x_4 \leq |\hat{x}| \leq x_5, \\[2mm] \frac{(k_7-k_6)\cdot(|\hat{x}|-x_5)}{(C-x_5)} + k_6, & \text{for } x_5 \leq |\hat{x}| \leq C. \end{cases}$$

The damper characteristics are defined similar to the spring characteristics in the model:

$$c(\dot{x}) = \begin{cases} \frac{(c_2-c_1)\cdot|\dot{\hat{x}}|}{\dot{x}_1} + c_1, & \text{for } |\dot{\hat{x}}| \leq \dot{x}_1, \\[2mm] \frac{(c_3-c_2)\cdot(|\dot{\hat{x}}|-\dot{x}_1)}{(\dot{x}_2-\dot{x}_1)} + c_2, & \text{for } \dot{x}_1 \leq |\dot{\hat{x}}| \leq \dot{x}_2, \\[2mm] \frac{(c_4-c_3)\cdot(|\dot{\hat{x}}|-\dot{x}_2)}{(\dot{x}_3-\dot{x}_2)} + c_3, & \text{for } \dot{x}_2 \leq |\dot{\hat{x}}| \leq \dot{x}_3, \\[2mm] \frac{(c_5-c_4)\cdot(|\dot{\hat{x}}|-\dot{x}_3)}{(\dot{x}_4-\dot{x}_3)} + c_4, & \text{for } \dot{x}_3 \leq |\dot{\hat{x}}| \leq \dot{x}_4, \\[2mm] \frac{(c_6-c_5)\cdot(|\dot{\hat{x}}|-\dot{x}_4)}{(\dot{x}_5-\dot{x}_4)} + c_5, & \text{for } \dot{x}_4 \leq |\dot{\hat{x}}| \leq \dot{x}_5, \\[2mm] \frac{(c_7-c_6)\cdot(|\dot{\hat{x}}|-\dot{x}_5)}{(v_0-\dot{x}_5)} + c_6, & \text{for } \dot{x}_5 \leq |\dot{\hat{x}}| \leq v_0, \end{cases}$$

where k is the front end spring coefficient, c is the front end damper coefficient, $\hat{x}$ is the computed vehicle deformation, $\dot{x}$ is the vehicle velocity, $\dot{\hat{x}}$ is the computed vehicle velocity, C is the maximum dynamic crush, v_0 is the velocity at the time of maximum dynamic crush. The optimization algorithm which minimizes the error between the test and computed values has been used to determine the acceleration, velocity and deformation of the vehicle. The error function is defined by $E(\Theta,t)$ in Eq. (3a) where Θ, which denotes the unknown variables in the mode. The validation data from FE model and optimization algorithm are plotted in Fig. 6.

$$E(\Theta,t) = E_1(\Theta,t) + E_2(\Theta,t) + E_3(\Theta,t), \text{where} \tag{3a}$$

$$E_1(\Theta,t) = |(a_{FE} - a_{LPM})| \tag{3b}$$

$$E_2(\Theta,t) = |(v_{FE} - v_{LPM})| \tag{3c}$$

$$E_3(\Theta,t) = |(x_{FE} - x_{LPM})| \tag{3d}$$

where, a is the acceleration; v is the vehicle velocity; and x is the displacement.

2.3. Governing equations of motion

The governing equations of motion for the vehicle impacting the barrier have been modeled using the relativistic Lagrangian formulation [22]:

$$\frac{d}{dt}\frac{\partial L}{\partial \dot{q}_i} - \frac{\partial L}{\partial q_i} + \frac{\partial D}{\partial q_i} = Q_i,$$

where, in general case, $L = T - V$, T is the total kinetic energy of the system equal to the sum of the kinetic energies of the particles, $q_i, i = 1, \ldots, n$ are generalized coordinates and V is the potential energy of the system. Here D is the dissipation function and Q_i is the external force acting on the system; in this case it is the vertical component of
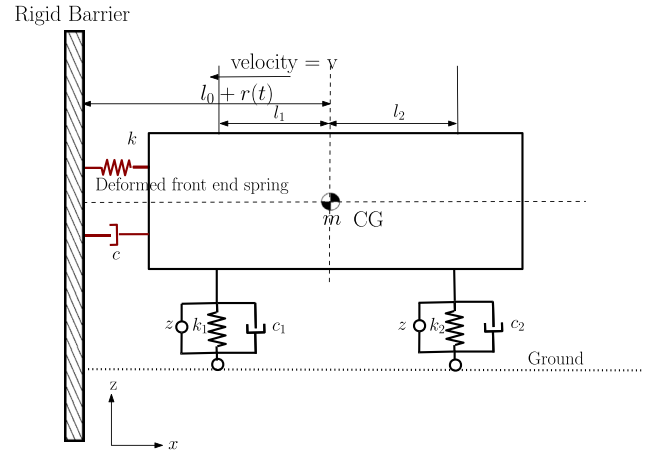

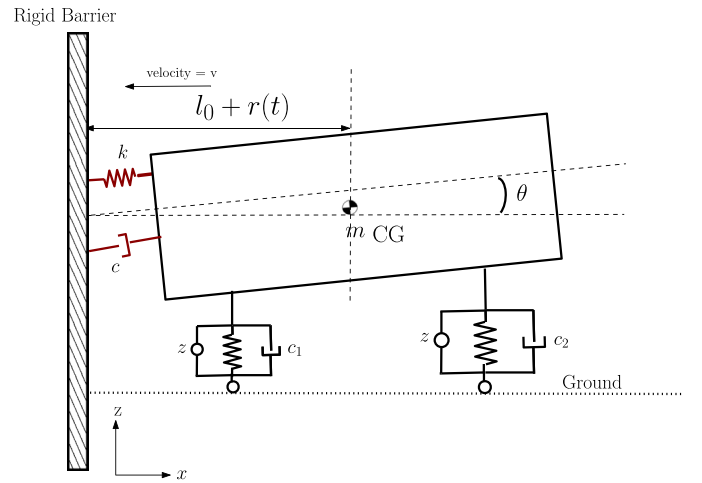Fig. 4. Vehicle front end members undergoing deformation.

Fig. 5. LPM representation of vehicle pitching forward in the event.
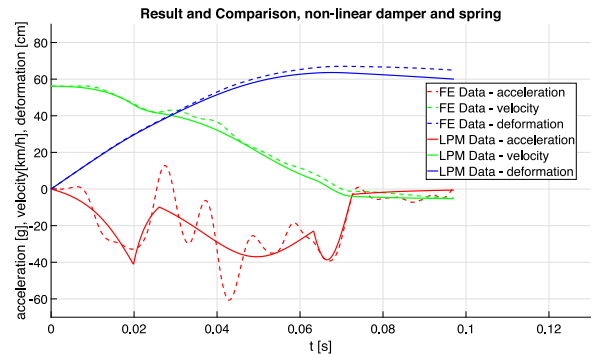
Fig. 6. Plot of computed and test values from parameterization algorithm.

the force experienced by the vehicle at the time of maximum dynamic crush [19].

For the purpose of simplifying the system, we converted the cartesian coordinates to polar coordinates: the horizontal (x) and vertical (z) coordinates and the angle of rotation θ about the y axis, were represented in polar coordinates by the following expressions:

$$x = [l_0 + r(t)]\cos\theta(t), \tag{4}$$

$$z = [l_0 + r(t)]\sin\theta(t), \tag{5}$$

where l_0 is the distance from the center of gravity (CG) to the point of impact of the vehicle at the rest position, $r(t)$ is the displacement along the polar radius of the elastic pendulum spring, t is the time, and r and θ are the radius and angle in polar coordinates respectively. Taking the derivatives of x and z with respect to time t we obtain:

$$\dot{x} = \dot{r}\cos\theta - (l_0 + r)\sin\theta \cdot \dot{\theta}, \tag{6}$$

$$\dot{z} = \dot{r}\sin\theta + (l_0 + r)\cos\theta \cdot \dot{\theta}, \tag{7}$$

where $\dot{x}$ and $\dot{z}$ represent the velocity of the vehicle in horizontal and vertical directions. Squaring both sides of the equations gives us:

$$\dot{x}^2 = \dot{r}^2\cos^2\theta + (l_0 + r)^2\sin^2\theta \cdot \dot{\theta}^2 \\ - 2\dot{r}\cos\theta \cdot (l_0 + r)\sin\theta \cdot \dot{\theta}, \tag{8}$$

$$\dot{z}^2 = \dot{r}^2\sin^2\theta + (l_0 + r)^2\cos^2\theta \cdot \dot{\theta}^2 \\ + 2\dot{r}\cos\theta \cdot (l_0 + r)\sin\theta \cdot \dot{\theta}. \tag{9}$$

Adding the terms we have:

$$\dot{x}^2 + \dot{z}^2 = \dot{r}^2(\cos^2\theta + \sin^2\theta) \\ + (l_0 + r)^2 \cdot \dot{\theta}^2(\cos^2\theta + \sin^2\theta). \tag{10}$$

The kinetic energy of the system is given by

$$T = \frac{1}{2}m(\dot{x}^2 + \dot{z}^2), \tag{11}$$

or, in polar coordinates,

$$T = \frac{1}{2}m[\dot{r}^2 + (l_0 + r)^2\dot{\theta}^2]. \tag{12}$$

The potential energy of the system can be found as

$$V = mg(l_0 + r)\sin\theta + \frac{1}{2}kr^2 + \frac{1}{2}k_1 r_1^2 + \frac{1}{2}k_2 r_2^2, \tag{13}$$

where r_1 and r_2 are expressed in terms of r and θ as follows:

$$r_1 = (l_0 + r - l_1)\theta, \tag{14}$$

$$r_2 = (l_0 + r - l_2)\theta. \tag{15}$$

Here m is the mass of the lumped body, l_1 is the distance from the CG to the front suspension, l_2 is the distance from the CG to the rear suspension. Simplifying the expression for potential energy in Eq. (13), we obtain:

$$V = mg(l_0 + r)\sin\theta + \frac{1}{2}kr^2 + \frac{1}{2}k_1(l_0 + r - l_1)^2\theta^2 \\ + \frac{1}{2}k_2(l_0 + r - l_2)^2\theta^2. \tag{16}$$

Here k_1 and k_2 are the suspension spring coefficients for the front and rear suspension respectively. Using Eqs. (12) and (16) and Lagrangian formulation, $L = T - V$, we conclude that

$$L = \frac{1}{2}m[\dot{r}^2 + (l_0 + r)^2\dot{\theta}^2] - mg(l_0 + r)\sin\theta - \frac{1}{2}kr^2 \\ - \frac{1}{2}k_1(l_0 + r - l_1)^2\theta^2 - \frac{1}{2}k_2(l_0 + r - l_2)^2\theta^2. \tag{17}$$

The governing equations of motion are:

$$Q_r^{ext} = m\ddot{r} - mr\dot{\theta}^2 - ml_0\dot{\theta}^2 + mg\sin\theta \\ + kr + \frac{1}{2}k_1(2r - l_0 r - l_1)\theta^2 \\ + \frac{1}{2}k_2\theta^2(2r + l_0 r + 2l_2), \tag{18}$$

$$Q_\theta^{ext} = m(l_0 + r)^2\ddot{\theta} + mg(l_0 + r)\cos\theta \\ + k_1(l_0 + r - l_1)^2\theta + k_2(l_0 + r + l_2)^2\theta, \tag{19}$$

where Q_r^{ext} and Q_θ^{ext} are the external forces experienced by the vehicle. The non-conservative forces experienced by the system are included in the Lagrange's equation of motion in the form of generalized forces expressed with the formulation of virtual work δU [15]:

$$\delta U = \sum_{j=1}^{m} F_j \cdot \delta r_j, \tag{20}$$

where F_j are the force components, δr_j are the virtual displacements given by

$$\delta r_j = \sum_{i=1}^{N} \frac{\partial r_j}{\partial q_i}\delta q_i \tag{21}$$

for $j = 1, 2, 3, \ldots, m$. This yields the following equation for virtual work as:

$$\delta U = F_1 \cdot \sum_{i=1}^{N} \frac{\partial r_j}{\partial q_i}\delta q_i + F_2 \cdot \sum_{i=1}^{N} \frac{\partial r_j}{\partial q_i}\delta q_i + \cdots \\ + F_m \cdot \sum_{i=1}^{N} \frac{\partial r_j}{\partial q_i}\delta q_i. \tag{22}$$

Using Eq. (22), we compute the generalized forces experienced by the system.

$$\delta U = F_x \cdot \left(\frac{\partial x}{\partial r}\cdot\delta r + \frac{\partial x}{\partial\theta}\cdot\delta\theta\right) \\ + F_z \cdot \left(\frac{\partial z}{\partial r}\cdot\delta r + \frac{\partial z}{\partial\theta}\cdot\delta\theta\right). \tag{23}$$

Substituting Eqs. (4) and (5) in Eq. (23), we get

$$dU = F_x \cdot [(\cos(\theta)\delta r - (l_0 + r)\sin(\theta)\delta\theta)] \\ + F_z \cdot [(\sin(\theta)\delta r + (l_0 + r)\cos(\theta)\delta\theta)]. \tag{24}$$

The external forces included in this LPM are barrier forces, damper forces including front end spring damper system and suspension damper system forces. The corresponding equations are:

$$Q_r^{ext} = Q_r^{bar} + Q_r^{damp}, \tag{25}$$

$$Q_\theta^{ext} = Q_\theta^{bar} + Q_\theta^{damp}. \tag{26}$$

Here F_x and F_z are the horizontal and vertical force components acting on the vehicle; Q_r^{bar} and Q_θ^{damp} are the non-conservative barrier and damper forces acting on the system.

Then δU becomes:

$$\delta U = Q_r^{damp} \cdot \delta r + Q_\theta^{damp} \cdot \delta\theta \\ + Q_r^{bar} \cdot \delta r + Q_\theta^{bar} \cdot \delta\theta, \tag{27}$$

where

$$Q_r^{bar} = F_{bx}\cos(\theta) + F_{bz}\sin(\theta), \tag{28}$$

$$Q_\theta^{bar} = -F_{bx}(l_0 + r)\sin(\theta) + F_{bz}(l_0 + r)\cos(\theta), \tag{29}$$

where F_{bx} and F_{bz} are the barrier forces experienced by the vehicle in the horizontal and vertical directions. These values are included from the FE simulation data. The derivative of the dissipation energy D is calculated and the damper forces are presented below:

$$Q_r^{damp} = F_{bx}\cos(\theta) + F_{bz}\sin(\theta), \tag{30}$$

$$Q_\theta^{damp} = -F_{bx}(l_0 + r)\sin(\theta) + F_{bz}(l_0 + r)\cos(\theta), \tag{31}$$

$$Q_r^{damp} = c\dot{r}\cos(\theta) + c_1[(l_0 + r - l_1) + \dot{r}\theta] \\ + c_2[(l_0 + r + l_2) + \dot{r}\theta]\sin(\theta), \tag{32}$$

$$Q_\theta^{damp} = -c\dot{r}(l_0 + r)\sin(\theta) + [c_1(l_0 + r - l_1)\dot{\theta} \\ + c_2(l_0 + r + l_2)\dot{\theta}](l_0 + r)\cos(\theta), \tag{33}$$

where c_1 and c_2 are the damper coefficients for the front and rear suspensions.

3. Results and discussion

The LPM was simulated in Simulink and the results were compared with the data generated from the FE model for a 2014 Chevrolet Silverado impacting a rigid barrier at 56 kmph. The curve outputs from LS Dyna were converted to polar coordinates before overlaying

Table 1
Automotive parameters set [23].

Symbol	Value	Unit	Meaning
M	400	kg	Sprung mass
m_{ij}	50	kg	Unsprung masses (i = front, rear and j = left, right)
I_x	250	kg.m^2	Roll inertia
I_y	1400	kg.m^2	Pitch inertia
t	1.4	m	Front and rear axle
l_f	1.4	m	COG-front distance
l_r	1	m	COG-rear distance
r	0.3	m	Nominal wheel radius
h	0.7	m	Chassis COG height
k_f	30,000	N/m	Front suspension linearized stiffness (left, right)
k_r	20,000	N/m	Rear suspension linearized stiffness (left, right)
c_f	1500	N/m/s	Front suspension linearized damping (left, right)
c_r	3000	N/m/s	Rear suspension linearized damping (left, right)
k_t	200,000	N/m	Tire stiffness (front, rear and left, right)
β	50	rad/s	Suspension actuator bandwidth

them with LPM results. The Simulink model was run with an ode 45 (fixed solver) and the change of the solver type did not improve or deteriorate the performance of the model. Prediction of the velocity of the vehicle after impact for the entire impact event is crucial for vehicle design in the development stages; in most cases the time of maximum crush coincides with the instant when the vehicle stops. The maximum crush (displacement) contributes to the energy absorbed by the front end members and is an important parameter for vehicle injury prediction. As described in the previous section, in a full vehicle impact scenario, the vehicle pitches forward which may lead to serious head and neck injuries to occupants. Vehicle pitch angle plays an important role in designing active safety measures like airbags by helping to mitigate occupant injuries. The pendulum inspired model developed in this study predicts these parameters; the maximum displacement of the vehicle in the LPM is overlayed with FE data in Fig. 7.

The values of k_1, k_2, c_1, c_2, l_1, l_2 and l_0 in Table 1 were taken from [23].

The vehicle deformation recorded from the LPM was plotted against the test data in Fig. 7. The maximum displacement in the vehicle front end is very closely correlated with the test data; this indicates that the prediction of vehicle deformation with model is accurate. The LPM curves, however, drop after 100 ms which can be attributed to the spring rebound in the model. The time the vehicle velocity becomes zero generally coincides with the instant for maximum crush making the prediction of velocity change on the vehicle an important parameter for improving crash performance. The curves comparing the test and LPM velocity curves show good correlation with close prediction of the time when the vehicle attains zero velocity as shown in Fig. 8. The vehicle pitching angle is an important parameter to determine the injury to occupants; the LPM and test curves were overlayed to observe acceptable prediction values of the pitching angle in Fig. 9. The vehicle rotations in the other axes were neglected in this study. The model over-predicts in case of pitching which can be addressed by taking into account spring rebound, however, the close correlation between the LPM and the FE data increases confidence in using LPMs for predicting occupant injuries in the future.

4. Conclusions

In this paper, we suggest a novel mathematical model for a full frontal vehicle crash. The following key aspects distinguish our model from those reported in the literature. First, instead of focusing on the pitching about the center of gravity as most existing models do, we simulate the vehicle pitching during a full frontal crash about the point of impact. Second, contrary to traditional approaches based on the use of Newtonian formulation [4,8] for the derivation of the governing equations of motion, we use relativistic Lagrangian formulation; the
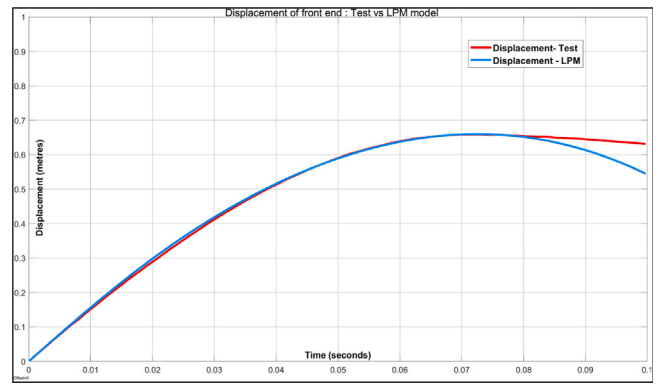

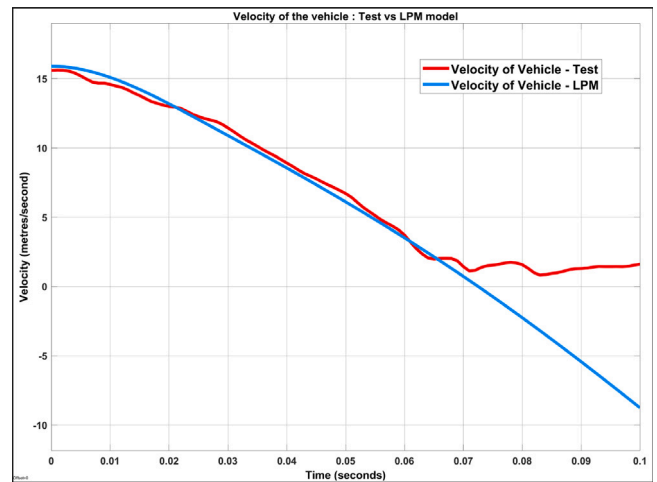**Fig. 7.** LPM simulation vehicle deformation curves compared with FE simulation data.

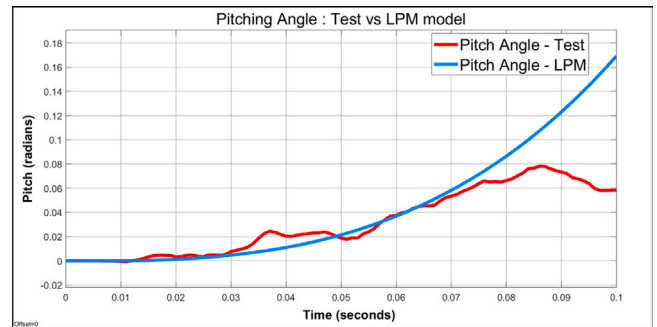**Fig. 8.** LPM simulation vehicle velocity curves compared with FE simulation data.

Fig. 9. LPM simulation vehicle pitching curves compared with FE simulation data.

model equations are further simplified by conversion to polar coordinates. The vehicle body pitches and drops at frontal impact are the main reason for the unbelted driver neck and head injury [6]. Third, we model the motion of the vehicle during the frontal impact as a rotation of a compound elastic pendulum about a pivot point; the pendulum uses a spring damper system for absorbing the impact energy. To our knowledge, there was no evidence of application of pendulum motion to model vehicle deformation and pitching in the literature making this a novel contribution of the work. An LPM model with 2 DOF designed in the paper has been simulated in Simulink. The results of the simulation correlate quite well with the data obtained in an FE simulation model developed by NHTSA. Since our model successfully replicates vehicle dynamics during the crash against a rigid barrier,

predicted parameter values for the front end deformation and pitching can be used by the automotive industry at initial stages of vehicle design.

Declaration of competing interest

The authors declare that they have no known competing financial interests or personal relationships that could have appeared to influence the work reported in this paper.

Data availability

Data will be made available on request.

References

[1] W. Weijermars, N. Bos, A. Schoeters, J.-C. Meunier, N. Nuyttens, E. Dupont, K. Machata, R. Bauer, K. Perez, J.-L. Martin, H. Johansson, A. Filtness, L. Brown, P. Thomas, Serious road traffic injuries in europe, lessons from the EU research project SafetyCube, Trans. Res, Rec. J. Transp. Res. Board 2672 (2018) 1–9, http://dx.doi.org/10.1177/0361198118758055, URL http://journals.sagepub.com/doi/10.1177/0361198118758055.

[2] G. Noorsumar, K. Robbersmyr, S. Rogovchenko, D. Vysochinskiy, Crash Response of a Repaired Vehicle - Influence of Welding UHSS Members, SAE International, 2020, http://dx.doi.org/10.4271/2020-01-0197.

[3] J.M. Chang, M. Rahman, M. Ali, T. Tyan, M. El-Bkaily, J. Cheng, Modeling and design for vehicle pitch and drop of body-on-frame vehicles, SAE Tech. Papers 114 (2005) 329–338, http://dx.doi.org/10.4271/2005-01-0356.

[4] A. Elmarakbi, M. Elkady, J. MacIntyre, Numerical analysis of vehicle-to-vehicle impact using vehicle dynamics control systems for collision mitigation, Int. J. Dyn. Control 1 (2013) 172–191, http://dx.doi.org/10.1007/s40435-013-0017-x.

[5] G. Noorsumar, S. Rogovchenko, K.G. Robbersmyr, D. Vysochinskiy, A. Klausen, A novel technique for modeling vehicle crash using lumped parameter models, in: Proceedings of the 11th International Conference on Simulation and Modeling Methodologies, Technologies and Applications, SIMULTECH 2021, SciTePress, 2021, pp. 62–70, http://dx.doi.org/10.5220/0010529200620070.

[6] J.M. Chang, M. Huang, T. Tyan, G. Li, L. Gu, Structural optimization for vehicle pitch and drop, SAE Tech. Papers (2006) http://dx.doi.org/10.4271/2006-01-0316.

[7] J.M. Chang, M. Ali, R. Craig, T. Tyan, M. El-Bkaily, J. Cheng, Important modeling practices in CAE simulation for vehicle pitch and drop, SAE International, 2006, http://dx.doi.org/10.4271/2006-01-0124.

[8] M. Elkady, A. Elmarakbi, J. Macintyre, Enhancement of vehicle safety and improving vehicle yaw behaviour due to offset collision using vehicle dynamics, Int. J. Veh. Saf. 6 (2012) 110–133, http://dx.doi.org/10.1504/IJVS.2012.049011.

[9] D. Benson, J. Hallquist, M. Igarashi, K. Shimomaki, M. Mizuno, Application of DYNA3D in large scale crashworthiness calculations, 1986.

[10] C.-S. Böttcher, S. Frik, B. Gosolits, 20 Years of crash simulation at opel-experiences for future challenge, 2005.

[11] M.M. Kamal, Analysis and Simulation of Vehicle to Barrier Impact, SAE International, 1970, http://dx.doi.org/10.4271/700414.

[12] B.B. Munyazikwiye, D. Vysochinskiy, M. Khadyko, K.G. Robbersmyr, Prediction of vehicle crashworthiness parameters using piecewise lumped parameters and finite element models, Designs 2 (2018) 43, http://dx.doi.org/10.3390/designs2040043.

[13] A. Deb, K.C. Srinivas, Development of a new lumped-parameter model for vehicle side-impact safety simulation, Proc. Inst. Mech. Eng. D 222 (2008) 1793–1811, http://dx.doi.org/10.1243/09544070JAUTO801.

[14] N. Pavlov, Study the vehicle pitch motion by spring inverted pendulum model, in: International Scientific Conference Mathematical Modeling,, 1, 2018, pp. 75–77.

[15] O. Cyrén, S. Johansson, Modeling of Occupant Kinematic Response in Pre-crash Maneuvers A simplified human 3D-model for simulation of occupant kinematics in maneuvers.

[16] S. Miao, Q. Cao, Modeling of self-tilt-up motion for a two-wheeled inverted pendulum, Ind. Robot 38 (2011) 76–85, http://dx.doi.org/10.1108/01439911111097878.

[17] M. Elkady, A. Elmarakbi, Modelling and analysis of vehicle crash system integrated with different VDCS under high speed impacts, Cent. Eur. J. Eng. 2 (2012) 585–602, http://dx.doi.org/10.2478/S13531-012-0035-Z.

[18] B. Han, Y. Oh, E. Lee, J. Lee, G. Kim, The effects of road contact angles and pitch/yaw angles on the injuries of drivers in CRIS test, in: 24th International Technical Conference on the Enhanced Safety of Vehicles (ESV) National Highway Traffic Safety Administration, (15–0350) 2015.

[19] G. Noorsumar, S. Rogovchenko, K.G. Robbersmyr, D. Vysochinskiy, Mathematical models for assessment of vehicle crashworthiness: a review, 2021, pp. 1–15, http://dx.doi.org/10.1080/13588265.2021.1929760,

[20] Crash Simulation Vehicle Models | NHTSA URL https://www.nhtsa.gov/crash-simulation-vehicle-models.

[21] A. Klausen, S.S. Tordal, H.R. Karimi, K.G. Robbersmyr, M. Jecmenica, O. Melteig, Mathematical modeling and optimization of a vehicle crash test based on a single-mass, in: Proceedings of the World Congress on Intelligent Control and Automation (WCICA), Vol. 2015-March, Institute of Electrical and Electronics Engineers Inc., 2015, pp. 3588–3593, http://dx.doi.org/10.1109/WCICA.2014.7053313.

[22] H. Goldstein, C. Poole, J. Safko, S.R. Addison, Classical mechanics, 3rd ed, Amer. J. Phys. 70 (2002) 782–783, http://dx.doi.org/10.1119/1.1484149, URL http://aapt.scitation.org/doi/10.1119/1.1484149.

[23] S. Savaresi, C. Poussot-Vassal, C. Spelta, O. Sename, L. Dugard, Semi-active suspension control design for vehicles, in: Semi-Active Suspension Control Design for Vehicles, Elsevier Ltd, 2010, http://dx.doi.org/10.1016/C2009-0-63839-3.